"The Application of the Jet Flap to Helicopter Rotor Control"

By R DORAND
(*Giravions Dorand*)

A meeting of the Association was held at the Royal Aeronautical Society, 4 Hamilton Place, London, W 1, at 6 p m on Friday, 6th November, 1959

Professor J A J BENNETT, (*Chairman of the lecture committee*) *occupying the Chair*

The CHAIRMAN, in opening the meeting, said that it was a pleasure to welcome at that meeting of the Association a distinguished engineer from France, Monsieur Rene Dorand, who was well known internationally as a pioneer of the helicopter M Dorand's name became associated with that of Louis Breguet in 1931 when they built in collaboration a helicopter with co-axial rotors That machine had achieved considerable success both in hovering and in forward flight It established international records for a flight duration of more than one hour and a forward speed of more than 100 k p h , and it also demonstrated an autorotative descent from 100 meters

M Dorand became a graduate engineer in 1921, and in the same year took a diploma in electrical engineering He then joined the Louis Breguet Aircraft Company as a graduate engineer and became Technical Director of the Breguet-Dorand Helicopter development group After the nationalisation of the aviation industry in France, he became Chief Engineer of the Societe Nationale de Constructions Aeronautiques de Centre, and later formed his own company, Giravions Dorand, of which he was now Technical Director The activities of the company included aeronautical research and the development of missile and flight simulators His pioneering work on helicopters was recognised a few months ago by the Royal Aero Club when he was awarded the Breguet Trophy for 1958

Mr Shapiro would read the paper and afterwards act as interpreter during the discussion

https://doi.org/10.1017/S2753447200004704 Published online by Cambridge University Press

THE APPLICATION OF THE JET FLAP TO HELICOPTER ROTOR CONTROL

Introductory Technical Considerations

Operators believe that the helicopter as a transport vehicle is too slow, too expensive and not very comfortable, due to its high level of vibration Is the application of the jet flap to the control of helicopter rotors capable of answering these criticisms ? This is what we are going to study here

Increase of speed

The main object aimed at is to make the helicopter capable of higher speeds First let us quickly survey the phenomena which limit the speed of existing helicopters

Air Compressibility

The permissible air speed at the blade tip is limited by the air compressibility, which imposes a reduction of the peripheral speed U when the flying speed V increases

Stalling

The air speed at the tip of the retreating blade, which is equal to the difference between the rotational speed and the flying speed V, decreases as the latter increases Therefore, the lift of the retreating blade can be maintained only by strongly increasing the lift coefficient C_L

The value of the maximum lift coefficient C_L is limited by stalling to about 1 2

Drawback of conventional cyclic control

The forward inclination of the axis of the cone swept by the blades becomes necessary at forward speeds so as to permit the projection on the speed vector V of the rotor thrust to overcome the combined drags of the rotor, the rotor head, and the fuselage as well as various parasite drags At high speeds this inclination becomes large

Due to this necessary inclination of the plane of rotation of the blades in a forward direction, the aerodynamic angle of incidence of the various sections of the blades, which depends on the translational and rotational velocity components triangle as well as the induced speed, varies as a function of the azimuthal position of the blade The variation follows as a geometric construction which results as a specific relationship or law between incidence and azimuth angle This law, which is badly adapted from the point of view of the aerodynamic angles of incidence of the profiles cannot be accurately corrected by the sinusoidal cyclic pitch variation imposed by the conventional type of control (forward inclination of the swashplate)

It must be pointed out that, for flying speeds of about 250 k p h the lift of a helicopter rotor is practically wholly provided by the blades as they pass through the plane of symmetry of the machine, the tip of the advancing blade even giving rise to a negative lift

Remedies envisaged

Two remedies have been envisaged for correcting these drawbacks of the helicopter rotor

Super-circulation (Cf references 1-A, 1-B, 3-A, 3-B)

The first solution consists in creating a super-lift effect at the tip of the retreating blade

https://doi.org/10.1017/S2753447200004704 Published online by Cambridge University Press

The application of this means alone (blowing air at the rear of the profile, suitably deflected jet flap) has for its purpose, by moving further away the limit of flow separation at the retreating blade to avoid the well-known loss of lift accompanying an increase of the speed

Compound harmonic control (Cf Ref 2)

The second solution consists in super-imposing on the conventional sinusoidal control a suitable compound higher harmonic control following a previously established ideal law adapted to the cruising speed

The higher harmonic blade pitch control encounters (1) mechanical design difficulties in embodying the course of the ideal control law as a function of speed, as well as (2) torsion stresses at the blade roots due to inertia loads caused by the higher harmonic law, which add to the torsional moments usually transmitted to the flying controls

Without the first remedy higher harmonic control would, however, theoretically give some advantages concerning improvement of the lift and of the lift/drag ratio of the rotor

Jet flap compound harmonic control

The aerodynamic conditions of economic use of the jet flap control require a suitable periodic adjustment of its deflection The higher harmonic actuation of the jet flaps requires practically no effort

Downward deflection of the flap moreover permits obtaining at the retreating blade tip very high C_L values (three times the stall C_L coefficient of unblown profiles

Principle of the jet flap control (Cf Ref 2-B, 4 and 6)

The pitch angle of the rotor blades is fixed at a given value which simplifies the rotor head Furthermore, the suppression of pitch variation permits a smooth passage of the air into the blades, which reduces internal circulation losses Each blade comprises but one single articulation that of vertical flapping motion The trailing edges at the blade tips are provided with an ejection slot for the driving fluid

Control is obtained by controlling the ejected fluid layer (jet flap) so as to deflect the same, which requires no effort on the part of the pilot, thus permitting in transport machines to dispense with servo-controls having a long time constant The simultaneous deflection of the jet flaps of the blades controls the total lift of the machine (vertical handling) (lever 14—Fig 4)

The periodic azimuthal deflection of the jet flaps performs the lateral and longitudinal control, in hovering flight, as well as translational flight (joy-stick 10—Fig 4)

A compound higher harmonic control, automatically adjusted as a function of the flying speed ensures the uniformity of the thrusts in all azimuths swept by the blades while reducing the vibration intensity

Aim of the paper

The purpose aimed at here is threefold (1) To show the conditions of jet flap control , (2) To report test results and their evaluation , and (3) To determine the practical applications of jet flap control examined from the point of view of transport economy for passengers and freight

Brief Description of a Jet Flap Rotor Control

Let us first describe the thermal jet driven rotor transport helicopter exclusively controlled by means of a jet flap

https://doi.org/10.1017/S2753447200004704 Published online by Cambridge University Press

The driving fluid supplied by a gas generator (hot or cold cycle) is expelled through trailing edge slots provided at the extremities of the blades

The blade pitch angle is fixed and each blade is provided with a single articulation (the conventional articulation for vertical flapping motion)

The rotorcraft control is performed solely by the adjustable action of the ejected driving fluid layer that constitutes the jet flap

Classification of Rotorcraft Equipped with Blade Trailing Edge Jets

Three classes of rotorcraft are distinguished

Class 1 *Class 1-A* *Helicopter provided with a mechanical power transmission drive*, the rotor of which embodies a minimum trailing edge jet flow sufficient only to ensure control of the boundary layer as well as to perform rotor control by means of a tangentially blown solid flap The shaft power of the compressor supplying the blade jets is about 15% of the total installed power on board the rotorcraft Cruising speed 270 to 300 km/h

Class 1-B Case of natural air blowing sustained by centrifugal circulation in the blades V = 260 km/h

Class 1-C Slotted flap V = 260 km/h

Note All Class 1 rotorcraft remain conventionally controlled

Class 2 *Thermal jet driven rotor helicopter* with a maximum air flow ensuring blade circulation control and thus rotor control by jet flap Cruising speed V = 280 to 330 km/h Piloting the rotorcraft is exclusively performed by means of the jet flap control

Class 3 *Rotorcraft with thermal jet driven rotor*, completely jet driven and jet flap-controlled, provided with an auxiliary propelling airscrew Cruising speed V = 350 to 390 km/h

Class 4 Same rotorcraft as above, provided with an auxiliary sustaining wing Cruising speed V = 370 to 430 km/h These machines are called " compound aircraft "

Remarks V designates the speed corresponding to economical operating costs

Comparison between the various rotorcraft classes Type of trailing edge control appropriate to every case

Class 1 Since the effectiveness of the trailing edge flap control is limited, the conventional cyclic control remains in use as well as collective pitch control

Classes 2 to 3 When the blade profile circulation is controlled—which is the case of interest here—the trailing edge flap alone (jet flap or composite flap solid and jet) is used for control (vertical handling, lateral and longitudinal controls, forward flight control)

Aerodynamic Advantages Brought about by the Higher Harmonic Flap Control

Reduction of the level of vibration In every case, the flap (either solid or constituted by a jet) undergoes, in forward flight, a higher harmonic control ensuring constancy, in all azimuths swept by the blades, of the aerodynamic thrusts moment, about the flapping hinge This method which

https://doi.org/10.1017/S2753447200004704 Published online by Cambridge University Press

suppresses the blade flapping motion of frequency $n\omega$, has the effect of reducing the level of vibration of the machine during translational flight

Increase of cruising speed This increase, which is about 20% for helicopters of Class 1, as compared with the conventional helicopter, reaches materially higher values for the other rotorcraft classes as defined previously

Increase of the mean C_L (C_{L_M}) *and the disc-loading* An increase of C_{L_M} results in reducing the solidity σ of the rotor and hence the power absorbed in forward flight by the profile drag

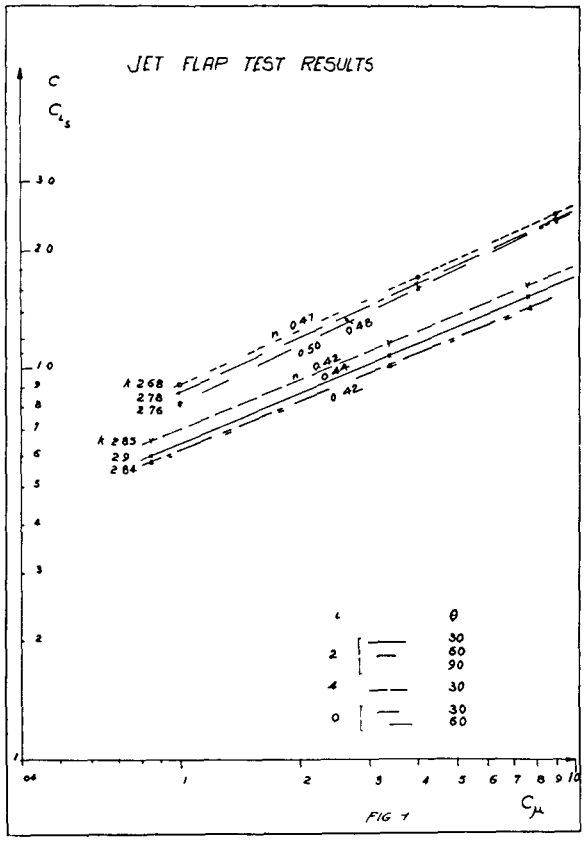

FIG 7

In the case of a Class 1 helicopter flying at a speed of 285 k p h , the disc-loading may reach, without any difficulty, 38 Kg/sq m

In rotorcraft of Classes 2 to 3, the disc-loading may reasonably reach 50 Kg/sq m

Reduction of the rotor drag The jet flow makes it possible to achieve lower rotor drag This drops from 5% of the aircraft weight in the case of the conventional helicopter down to 2% in the case of a Class 1 helicopter

In the case of Class 2, the jet flap control increases the propulsive effect of the rotor to the extent stated below and makes flight in the helicopter condition more attractive

https://doi.org/10.1017/S2753447200004704 Published online by Cambridge University Press

Improvement of the rotor lift/drag ratio f In the case of the helicopter, the lift/drag ratio of the rotor may be defined as the ratio of the product Fz × V to the power absorbed by the rotor for producing the lift and overcoming its own drag (Fz = vertical thrust of the rotor)

It must be pointed out in passing that even in the case of Class 1 helicopters, a gain in the lift/drag ratio is observed f increases from 5 85 (conventional rotor) to 7 6 (Class 1 helicopter flying at 285 K p h

The gross gain reaches 30% The net power gain is actually only 12% for the whole aircraft, if the efficiency of the pneumatic power transmission and the anti-torque losses are taken into account

Jet flap control increases more sharply the lift/drag ratio of the rotor which may reach the optimum value f = 11 5 for Class 2 helicopters with maximum jet flow

Recapitulation of the Properties of Control by Blown Flaps and Jet Flaps

Computation of the C_L coefficient in the case of a wing having an infinite aspect ratio

$$(1) \qquad C_Z = 2\pi i + KC\mu^n (i + \theta) + C\mu (i + \theta)$$

i = aerodynamic angle of incidence referred to the zero lift line (radians)

θ = downward deflection of the fluid (radians)

$C\mu$ = momentum coefficient

Experimental families of curves give K and n for each type of flap as a function of i and θ

Remarks The increase of $\frac{dC_L}{di}$ whose value is $KC\mu^n + C\mu$ explains

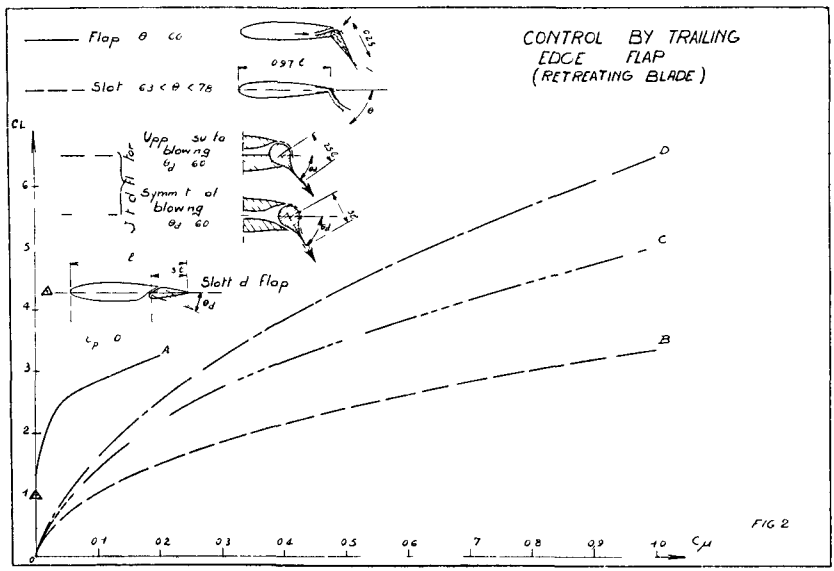

FIG 2

https://doi.org/10.1017/S2753447200004704 Published online by Cambridge University Press

the partial improvements sometimes obtained without any flap control

Case of the jet flap Fig 1 gives an example of a family of curves applied to the case of the jet flap limited to the numerical values of $C\mu$ relating to rotors of Classes 2 and 3 rotorcraft

θ geometric deflection (without wind)
θ' aerodynamic deflection (with wind)

Comparison between the various types of flaps or jet controls in the case of the retreating blade (deflection $\theta_d \neq 60°$) (Fig 2)

Solid flap with tangential air blowing (curve A) (Class 1) *Jet flap* (curve B)

(Classes 2 to 3) *ONERA jet controls*
with symmetrical air blowing (curve C),
with suction side air blowing (curve D)

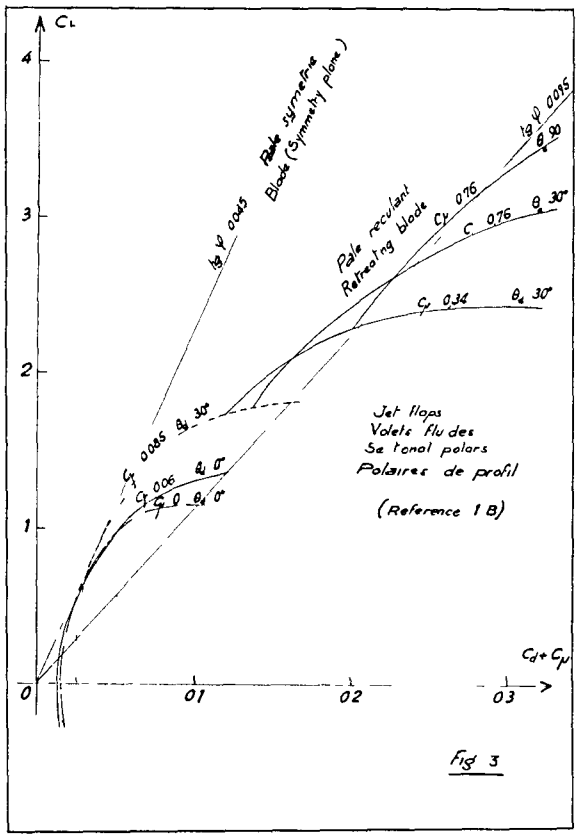

Composite controls (mechanical flaps provided with air blowing) (Groups 1 to 3) The effectiveness of these controls corresponds to that area of the diagram which is included between curves B and D Their use is essential when the effectiveness of the jet flap alone is insufficient (section between $r = 0\,6$ and $r = 0\,8$ or case of a high pressure ratio fluid)

https://doi.org/10.1017/S2753447200004704 Published online by Cambridge University Press

Polar curves of profiles with jet flap (Fig 3) The polars are plotted against $C_d + C\mu$ They include only a few results of measurement directly related to the subject of this paper

Case of a moderate flap deflection (Blade passing through the plane of symmetry in front of the rotorcraft)

An optimum lift/drag ratio f is obtained for $C_L = 0\,9$ (actual C_L with air blowing), namely, $f = 23$ as compared with $f = 21\,5$ (unblown profile)

Effect of Mach number on profiles provided with blown trailing edges A Mach number $M = 0\,85$ at the advancing blade tip is recommended It permits to take advantage of a C_L increase ΔC_L for the advancing blade by means of a slight flap deflection ΔC_L may reach 0 25 compared with an unblown profile without fear of compressibility effect (see blown flap tests within the transonic speed range, references 1-C and 3-B)

Control by Jet Flap

A diagrammatic embodiment drawing is necessary to understand the following discussion

Fig 4 shows diagrammatically two cross sectional views at right angles of the head of a thermal-jet driven rotor provided with jet flap control

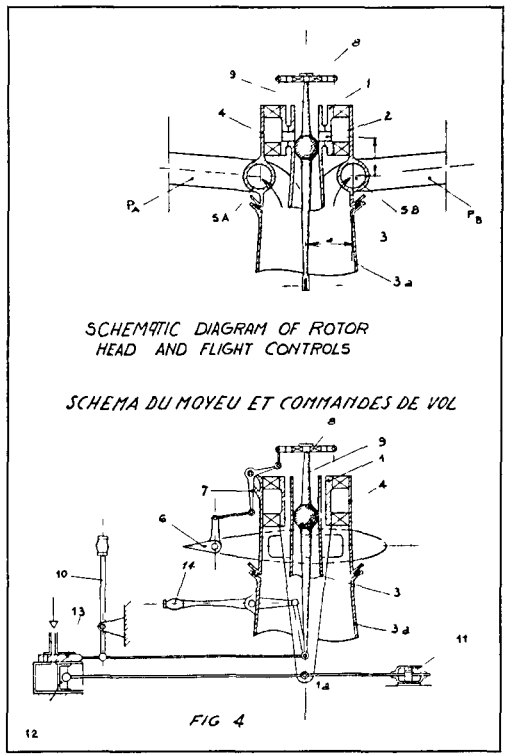

The table (Fig 4a) states by way of example, the conditions in translational flight at a speed of 290 K p h under blade pitch control, with a fixed flap (Case A) and under jet flap control with a fixed blade pitch (Case B)

https://doi.org/10.1017/S2753447200004704 Published online by Cambridge University Press

COMPARISON OF BLADE ANGLE CONTROL WITH JET FLAP CONTROL

TYPE OF CONTROL	(CLASSICAL) BLADE ANGLE CONTROL		JET FLAP CONTROL (NEW)		REMARKS
Airspeed V km/H	0	290	0	290	Speed attainable only with jet
Parameter μ	0	0,4	0	0,4	
General blade angle of attack θ	8	11	8	8	
Rotor head tilting: Rotor head pivot θ_0	0	5°3	0	8°3	Forward inclination as against normal for speed V
Virtual axis d_y	0	3 5	0	5 3	
Resultant F_x	0	3°5	0	3 5	
Cyclic control θ_z	0	7	0	0	Long fuselage control. By reducing amplitude e_3 from $r=0,5$ to $r=1$ the lift/drag ratio of the rotor would be improved (Solution of the future)
Flap deflection θ_d r 0,7 Advancing	0	0	0	3	
Symmetrical position	0	0	0	13	
Retreating θ_{dR}	0	0	0	43	
Amplitude of flapping motion and tilting of virtual axis about R	0	0	3	3	Alternating flexing of blades in the r plane (pulsations 2w) not transmitted to the pylon (Special arrangement of blade articulations)
Theoretical break-down of thrust in the case of fixed blades. This break down is changed in case A owing to the vertical flapping movement	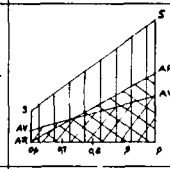		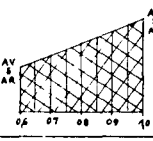		Source of vibrations with classical controls only cyclic deformations of blades by vertical bending and flapping motion nw (n > 1)
Azimuthal changes of aerodynamic moment at blade root. Predominant pulsations	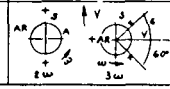		Constant moment flapping motion around nw (n > 1)		Flapping motions around nw ensure equilibrium but affect the lift/drag ratio of the rotor

FIG 4 bis

Description of the rotor head (shown two-bladed) The non-rotating portion 1 of the rotor head is articulated about a hinge, 2 parallel to the pitching axis, carried by the pylon 3

Each blade P_A and P_B is attached to the rotating portion 4 of the rotor head by a flapping articulation, 5_A and 5_B, respectively

The jet flap is diagrammatically shown in the shape of a conventional flap 6 In fact, it is mechanically controlled by a cam device embodying the ideal compound harmonic control law at the cruising speed This gear is diagrammatically shown in the shape of a lever 7

In the case of the DH-G 5 rotor as described later in the paper, the control was pneumatic and the flap was replaced by a deflecting rubber surface using the COANDA effect

The lever 7 is actuated by a small rotating swashplate 8 carried by a type of universally swivel mounted stick 9, vertically controlled by the collective flap deflection adjusting control organ 14 associated with both blades flaps (vertical flight control) Laterally and longitudinally the stick 9 is controlled by the joy-stick 10

Hovering flight control (Ref 7) However, the longitudinal control includes a servo-system the plane of rotation of the rotor head 1 follows the swashplate 8 controlled by the joy-stick It is to be noted that the flap 6 is cyclically controlled only during the transient period of applying control Tests carried out on a training simulator have shown that this arrangement leads to greater ease of piloting

Longitudinal control in forward flight (Ref 7) The aerodynamic conditions of the operation are such that the swashplate 8 progressively noses down relative to the rotor head as the speed increases The pneumatic cam which is shown diagrammatically in the shape of the lever 7 progressively and automatically comes into operation and produces compound higher

harmonic control of the flap In addition, it is beneficial from the aerodynamic point of view to cause a forward inclination by about 3° of the rotor head in relation to the plane of rotation of the articulated blades so as cyclically to correct the incidence For this purpose, the pneumatic reaction of the piston 12 is used which tilts the rotor head forward by about 3° in relation to the said plane of rotation

Comments on Table 4a Table 4a contains information to illustrate the following comments When changing from hovering flight to longitudinal flight the pitch may be fixed in the case of jet flap control while it has to be strongly increased in the case of blade angle control This table diagrammatically shows the considerable periodic variations in the thrust distribution, causing alternating flexure of the blades in the case of blade pitch control as compared with the case of jet flap higher harmonic control which practically suppresses all causes of vibration of the rotor

The aim of our discussion is to examine the aerodynamic conditions relating to the jet flap control as described above

Control of the vertical handling of the helicopter and control of the rotor lift The lever 14 controls the collective deflection of the flaps It is substituted for the conventional blade angle control when this is suppressed

A 5° jet flap deflection is equivalent to a 1° blade angle variation

The jet flap control effectiveness seems to be sufficient for obtaining either vertical take-off after having run up the rotor to overspeed (jet flaps brought back to zero after having been deflected upwardly at the time of the rotor starting) or flattening out in landing (jet flaps deflected downward by 40°)

Control by jet flap servo-action in hovering flight

Steady state-transient state The presence of the articulation 2 interconnecting the non-rotating portion of the rotor head to the rotor pylon permits the tilting axis of the rotor to follow by servo-action the tilting axis of the swashplate, the jet flap then acting, so to speak, as the oil control valve of a hydraulic servo-control

In a steady state, the deflection of the jet flap is constant in all azimuths and the oil control valve returns to zero

It is only in an unsteady state, during the transient periods of control that periodic motion of the flaps takes place whose total amplitude may reach 30°, which corresponds to variations of the aerodynamic angle of incidence by 6° as encountered in the case of conventional control

Control by jet flap at cruising speed

Double control Although the control column only controls the jet flap deflection a double aerodynamic control action takes place, which is shown on Table 4a

Profile incidence control due to tilting of the virtual axis relative to the rotor head axis We have seen that the fact of strongly pushing the joy-stick forward (cruising speed flight) causes tilting by about 3° of the rotor head axis relative to the virtual axis This tilting gives rise to an aerodynamic cyclic variation of the profile incidences which permits orienting the same correctly in the relative wind, incidence variations due to combination of the flying speed V, the local speed $\omega R\bar{r}$ and the induced speed V_i being taken into account This adaptation which requires no precision has the sole

https://doi.org/10.1017/S2753447200004704 Published online by Cambridge University Press

purpose of keeping the blade profile angles of incidence between convenient limits from 0 to 5° for the advancing blade and from 5 to 10° for the retreating blade

Jet flap higher harmonic control

Aim of flap control It is possible and advantageous to vary the periodic control law along the radius Flap sections would be operated separately, each one of them being provided, if required, with its own cam This kinematic arrangement has the purpose of ensuring so far as possible the constancy of the thrusts acting on the blade elements in all swept azimuths and hence to reduce the periodic deformations of the blades and, in particular, to ensure constancy of the moments resulting from the thrusts about the vertical flapping hinge

Example By way of illustration, we have shown a plot of the deflection law of a jet flap at a distance $\bar{r}R$ from the rotor head axis The local tip speed ratio has the value $\Lambda = 0\,4$

Observations concerning the variation of the incidence angle In the case of a flight in the helicopter condition, the profile incidence first decreases by an amount $\varphi\bar{r}$ due to forward tilting α_V of the virtual axis, according to a complex geometric law defined by the relation (2)

$$(2) \qquad \operatorname{tg} \varphi_{\bar{r}} = \frac{\Lambda_{\bar{r}} \left(\alpha_v + \frac{V_i}{V} \right)}{1 + \Lambda_{\bar{r}} \sin \Psi}$$

Evaluation of the aerodynamic incidence in the case of a conventional rotor not equipped with a jet flap A close study of this case is necessary to evaluate the faults of conventional cyclic control

Ideal case Let us first examine the ideal case of super-circulation

This case postulates the absence of stalling of the retreating blade profile

The curve A (Fig 5) is an example of a law for the incidence i_1 by which a constant thrust in all azimuths can be obtained

The arbitrary numerical data of this computation relate to a section at $\bar{r} = 0\,8$ of a helicopter whose advance ratio is $\Lambda = 0\,32$ with a very thin fuselage

$$\theta_c = 8^\circ \qquad \Lambda_{\bar{r}} = 0{,}4 \qquad \alpha_v + \frac{V_i}{V} = 0{,}10 \text{ radian}$$

The ideal law $\theta_2(\psi)$ of the complex harmonic control adapted to ensure constancy of the thrusts in all azimuths is embodied by curve B which looks like the sinusoidal curve C (conventional cyclic control) only within the half circle swept by the advancing blade As for the retreating blade, the ideal control amplitude ought to be four times greater than the cyclic control amplitude

Case of "stalling" The broken line section of curve A where i_1 exceeds

https://doi.org/10.1017/S2753447200004704 Published online by Cambridge University Press

the stalling incidence i_{d_s} shows that the lift loss already reaches 40% for $\bar{r} = 0\,8$ This loss substantially exceeds this value in the vicinity of the inversion circle

Case of jet flap control

Orientation of the profile in the relative wind With the same numerical

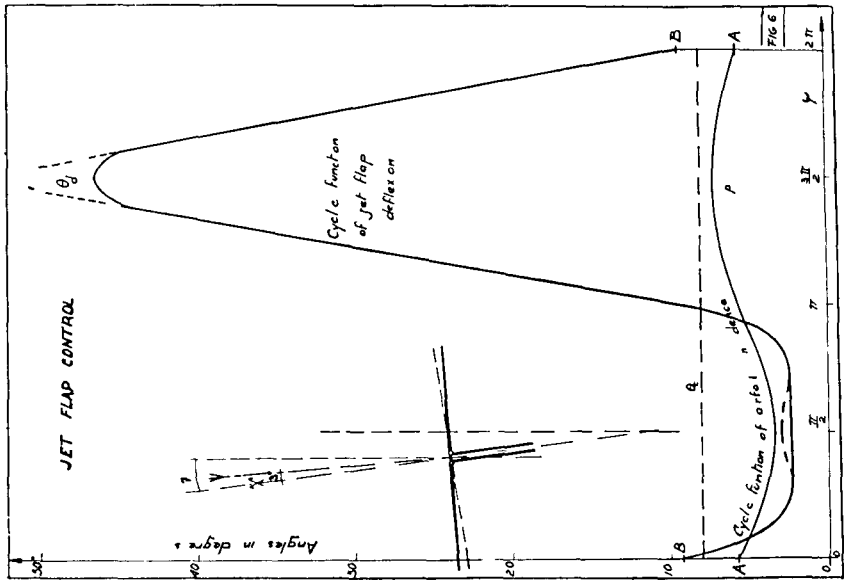

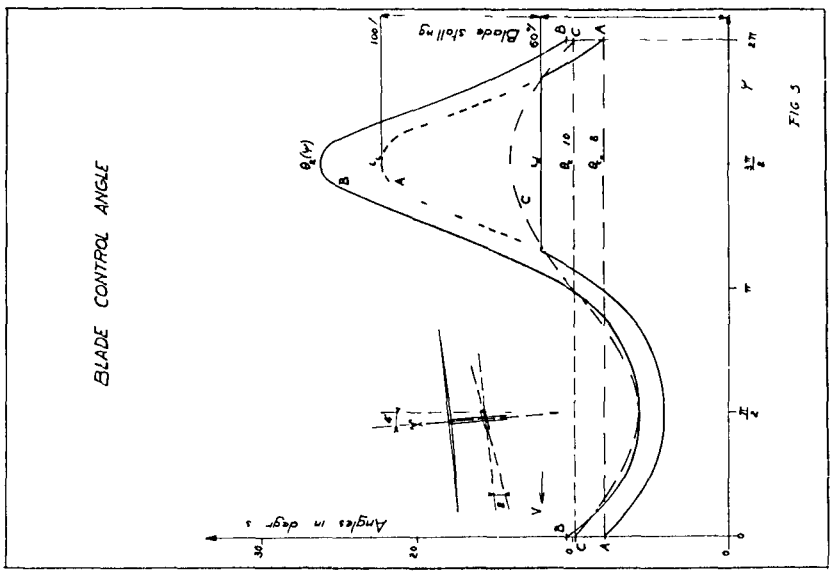

https://doi.org/10.1017/S2753447200004704 Published online by Cambridge University Press

data as above and arbitrarily assuming a tilting by 3° of the virtual axis backward from the rotor head axis, the law of evolution of the profile incidence i_p is first established This law is embodied by curve A (Fig 6)

The orientation of the profile in the wind is acceptable The tilting of 3° is reasonable Now the flap is introduced

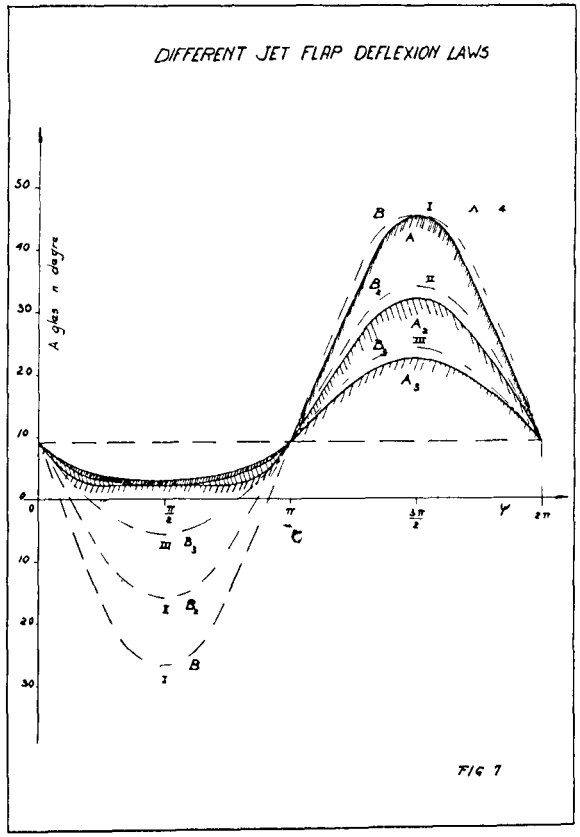

Flap control The deflection θd of the flap should, in combination with the profile incidence i_p, yield the C_L law defined by curve i_1 (Fig 5) This condition is expressed by the relation (3)

$$(3)\quad C_L = 2\pi i_v = (2\pi + K C_\mu^n) i_p + K C_\mu^n \theta_d$$

With the basic numerical data relating to the unblown reference rotor, and assuming $C\mu_o$ has its usual value ($C\mu_o$ = 0 1), the deflection law θd (curve B of Fig 6) can be drawn

Variation of periodic control law of the flap as speed decreases The diagram (Fig 7) shows the variation of the periodic control law of the

flap (curves A_1, A_2, A_3) as a function of the deflection of the swashplate (sinusoidal curves B_1, B_2, B_3), whose amplitude decreases with speed Curves A progressively look more and more like sinusoidal curves as the speed decreases

Embodiment of the flap deflection law Several fluid layer deflecting devices as well as mechanical and pneumatic jet control means adapted to various blade systems are now being tested under actual operating conditions

We shall give an example of the type of pneumatic deflector that has been found satisfactory during the test programme of the Dorand H-G 5 rotor carried out by O N E R A in the big Chalais-Meudon wind-tunnel

Favourable effect of large lift of the retreating blade on performance This analysis is necessary to understand the reason for the improvements observed during the tests of the DH-G 5 rotor

Instantaneous local lift/drag angle and instantaneous local relative propulsive force The knowledge of these ratios permits a full statement of the qualities of the rotor by a double integration along the radius and azimuthally

Local lift/drag angle (4) , Relative propulsive force (5)

$$(4) \qquad \operatorname{tg} \varphi_s = \frac{W_s}{F_z V}$$

$$(5) \qquad \operatorname{tg} \varphi_F = \frac{F_x}{F_z}$$

W_s is the power absorbed by the rotor to sustain the lifting force F_z and overcome its own drag

F_x propulsive component of the rotor supplying to the fuselage a power W_F given by the relation (6)

$$(6) \qquad W_F = F_X V$$

The total power supplied to the rotor W_R thus has the following value (7)

$$(7) \qquad W_R = W_S + W_F$$

Comparison between the local lift/drag ratios and relative propulsive forces of the retreating blade and the blade passing through the plane of symmetry These two trigonometric ratios are given by the approximate relations (8) and (9) which hold good for the purposes of comparison to be made

$$(8) \qquad \operatorname{tg} \varphi_{sF} = \frac{1}{\lambda_R^2} \frac{C_{D_P}}{C_L} + \sin \psi \frac{C_{D_P}}{C_L} + \frac{V_L}{V}$$

https://doi.org/10.1017/S2753447200004704 Published online by Cambridge University Press

$$(9)\qquad \operatorname{tg}\varphi_{F\bar{r}} = \frac{\alpha}{1+\Lambda_{\bar{r}}\sin\psi} - \sin\psi\,\frac{C_{DP}}{C_L} - \sin\psi\,\frac{\Lambda_{\bar{r}}\,\frac{V_1}{V}}{1+\Lambda_{\bar{r}}\sin\psi}$$

C_{D_P} is the profile drag

Numerical application to the azimuth of symmetry and the retreating blades The ideal incidence curve (Fig 5) gives, when multiplying i by $\frac{dC_L}{di}$, the instantaneous C_I value

The polar curves (Fig 3) give the following C_L and $\frac{C_{D_P}}{C_L}$ values

Blade	*Symmetry*	*Retreating*
C_L	0 80	2 20
$\frac{C_{DP}}{C_L}$	0 045	0 075

Let us take for α_V, the value $\tan\alpha_V = 0\ 10$,
and now for $\frac{V_1}{V}$, a mean value $\frac{V_1}{V} = 05$

Let us remember that the value of $\Lambda_{\bar{r}}$ is $\Lambda_r = 4$
The numerical example used for the relations (9) (10) gives the following values

	Azimuth	*Symmetry*	*Retreating*	*Observ*
Blade	Sin ψ	0	—1	
Lift/drag ratio	tan φ_{Sr}	163	162	Same value
Relative propulsive force	tan φ_{Fr}	10	27	Superiority of retreating blade

In spite of the increase of the profile drag, the retreating blade offers the same lift/drag ratio as the blade passing through the plane of symmetry owing to the reduction of the air speeds It does not affect the lift/drag ratio of the rotor Moreover, it gives rise to a forward force which contributes to propulsion of the helicopter

The ratio between the propelling forces due to the retreating blade and the blade passing through the plane of symmetry is always above 2 in the case of optimum flap control, as indicated by expression (10)

https://doi.org/10.1017/S2753447200004704 Published online by Cambridge University Press

$$(10) \qquad \frac{F_{x_{AR}}}{F_{x_S}} = 2 + \frac{\frac{V_L}{V} + \frac{C_{D_P}}{C_L}}{\alpha_V}$$

Aerodynamic conclusions The jet flap complex harmonic control ought to permit increase of the tip speed ratio, the speed, and the lift/drag ratio of the rotor as well as its propulsive force, thus benefitting flight in the pure helicopter conditions

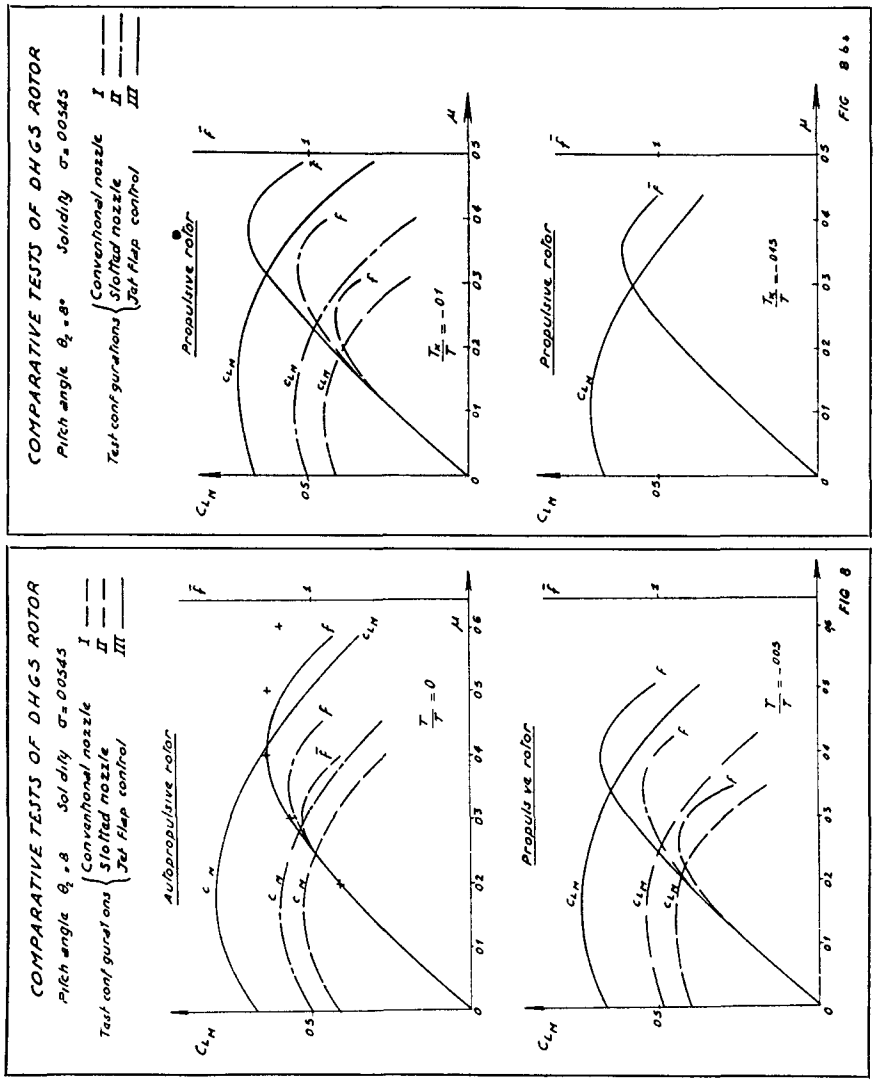

https://doi.org/10.1017/S2753447200004704 Published online by Cambridge University Press

Experimental Confirmation of these Conclusions according to the Tests of the Dorand H-G 5 Rotor carried out in the big Chalais-Meudon Wind-Tunnel (Ref 3-B and 6)

Characteristics of the rotor

Diameter		$D = 6,^{m}50$
Solidity		$\sigma = 0545$
Blade angle	=	$\theta_c = 8^-$

Compared configurations of the rotor with removable blade tip

Conventional elliptic nozzle and control by conventional swashplate (blade pitch control)

Ejection slot whose width increases towards the blade tip, extending from 70% of the radius to the end of the blade tip (jet flap with fixed deflection) and conventional swashplate control (blade pitch control)

Ejection slot as above with jet flap control (controlled deflection of the jet flap within a zone comprised between 86% of the radius and the end of the blade tip Deflection 10° for the advancing blade, 33° for the retreating blade)

Results The graphs (Figs 8 and 8a) show that the jet flap permits increasing compared to the case of the conventional rotor, the cruising speed V corresponding to the optimum lift/drag ratio (increase of the advance ratio) as well as increasing the blade-loading (increase of the mean lift coefficient C_{L_M}), and the rotor lift/drag ratio $\overline{f}$ (f is the ratio between the measured lift/drag ratio and the optimum lift/drag ratio of a conventional helicopter) while further reducing the rotor drag (increase of the rotor propulsive force)

Curves 1-A relate to the specific case of a self-propelling rotor

Curves 1-B, 1-C, 1-D, relate to the specific case of a rotor generating a propulsive force F_X to pull the fuselage corresponding to 5, 10 and 15% of the helicopter weight

The gain is substantially greater in the case of jet flap control

The crosses indicate the results of the application of the usual project study methods

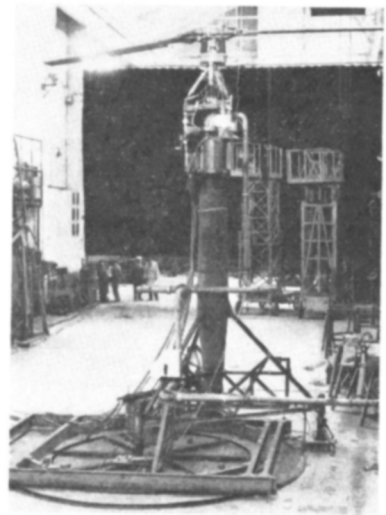

Fig 9

Experimental Details concerning Jet Flap Control

General view of the testing plant for the DH-G 5 rotor The photograph (Fig 9) shows a general view of the rotor together with its electrical measuring equipment whose dynamic readings were transmitted by means of O N E R A slip rings and recorded in the test control room equipped with new high precision O N E R A instruments (Characteristics of the fluid

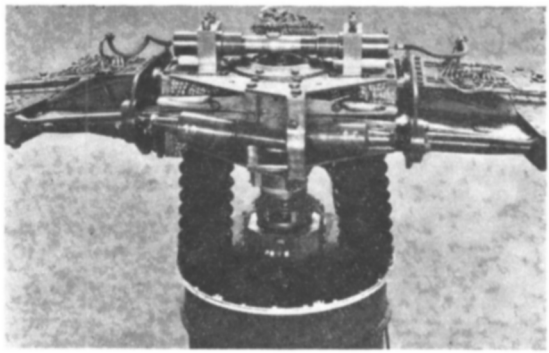

Fig 10

circulating through the blades, flap deflection law, flexure and torsion strains of the blade aerodynamic components, speeds, etc)

Pneumatic jet flap controlling system

Modulated pressure generating unit The photograph (Fig 10) shows the air pump (valveless) associated with the rotor head and actuating the pneumatic flaps

Pneumatic flap Fig 11 shows the principle of the pneumatic flap control by guiding the air layer by means of an inflatable rubber surface as well as the results of deflection efficiency measurements carried out at the Saint-Cyr laboratory

Fig 11a shows a combination of mechanical and jet flaps

Embodiment of the jet flap deflection laws by applying positive and negative pressures Air-pump adjustment parameters off-setting the centre line of the connecting rod attachment with respect to the rotor head axis, positional adjustment of the admission ports of the cylinders which rotate with the rotor head

The photograph (Fig 12) shows a visualization by means of wool tufts of the periodic deflection of the flap

The photograph (Fig 13) shows a recording of a flying control law approaching that of Fig 7

Examples of test results providing a comparison between the three following configurations conventional nozzle, slot nozzle with fixed deviation, jet flap control

Sample measurements The comparative graphs of these three configurations (Fig 14) show, as found by measurements, carried out on the same rotor with the three configurations, in which proportion the gains predicted confirmed and demonstrated, can be obtained when changing from the conventional nozzle to jet flap control

Comparison of the measurements These diagrams actually show the following result

Increase of lift (F_Z), propulsive force $\frac{F_X}{F_Z}$ and lift/drag ratio for the same advance ratio Λ above the usual values ($0\,3 < \Lambda < 0\,4$)

Increase of the ratio Λ for same values of C_L and the rotor lift/drag ratio

https://doi.org/10.1017/S2753447200004704 Published online by Cambridge University Press

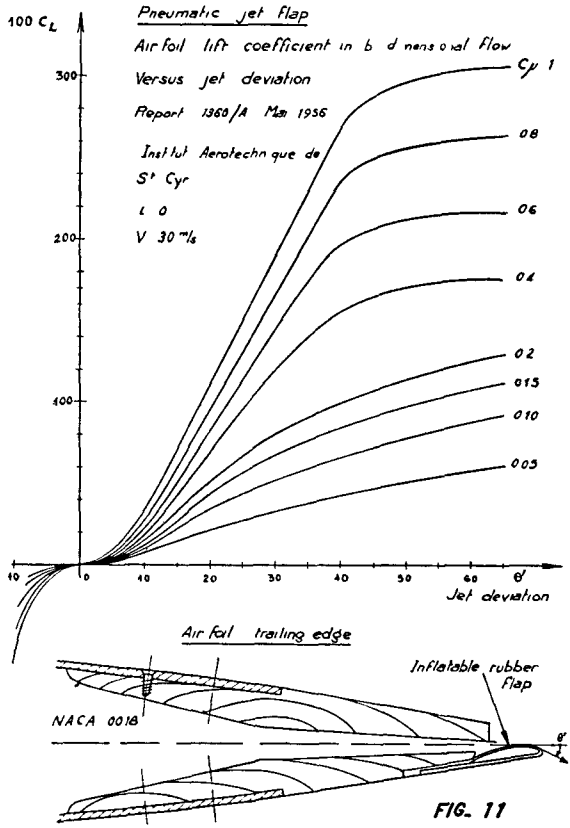

FIG. 11

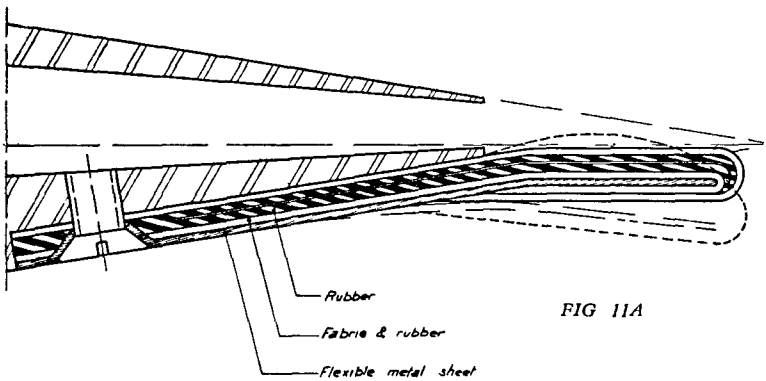

FIG 11A

https://doi.org/10.1017/S2753447200004704 Published online by Cambridge University Press

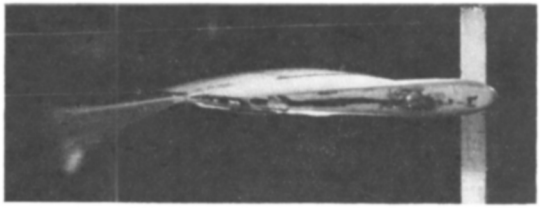

Fig 12

High values of the advance ratio $\Lambda = 0\ 7$ have been reached without giving rise to any vibrations

Possibility of reaching exceptionally high lift values The diagram (Fig 15) shows that, by progressively deflecting the mean position of the flap up to 40°, high values of C_{L_M} (1 5 as against the usual value of 0 4) can be reached in forward flight ($\Lambda = 35$)

The optimum value of f corresponds to about $C_{L_M} = 9$ for a flap deflection of 10°

Comparative summary table of the three configurations (*Fig 16*) (*a*) Case of flight with optimum lift/drag ratio of the rotor, (*b*) Case of maximum propulsive force

Test results in the case of jet flap control The diagram (Fig 17) shows as a function of the advance ratio Λ, the corresponding values of the lift/drag ratio $\overline{f}$, of the mean C_L (C_{L_M}) and the relative horizontal component of the rotor

Lift/drag ratio corrections Corrections for solidity, profile drag and Reynolds number are required, the reduction of σ and C_{D_p} improving the lift/drag ratio The first two conditions have been incorporated in the computation relating to the following study

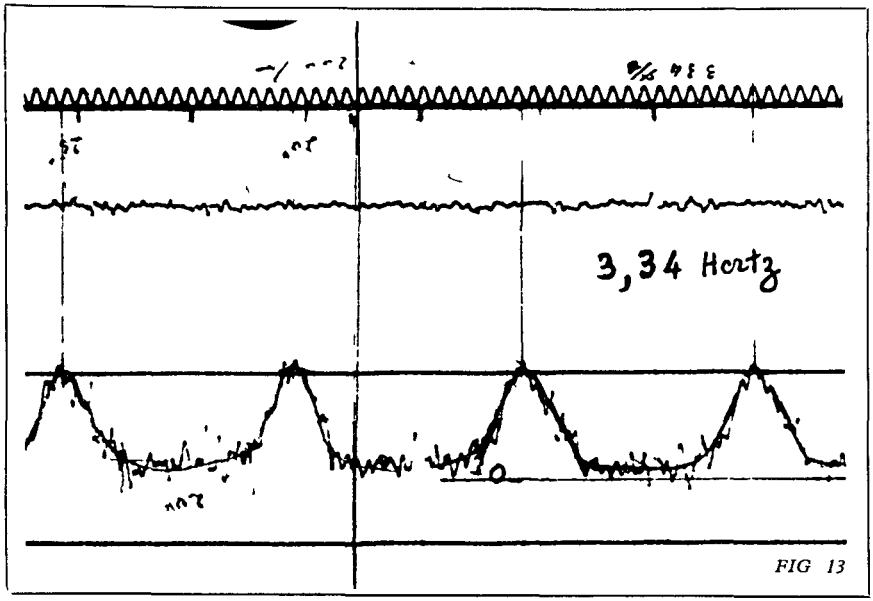

FIG 13

https://doi.org/10.1017/S2753447200004704 Published online by Cambridge University Press

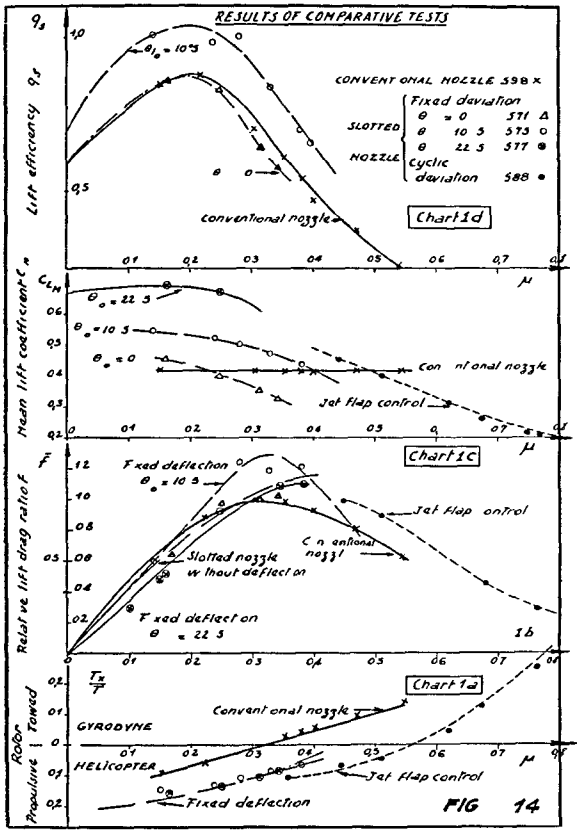

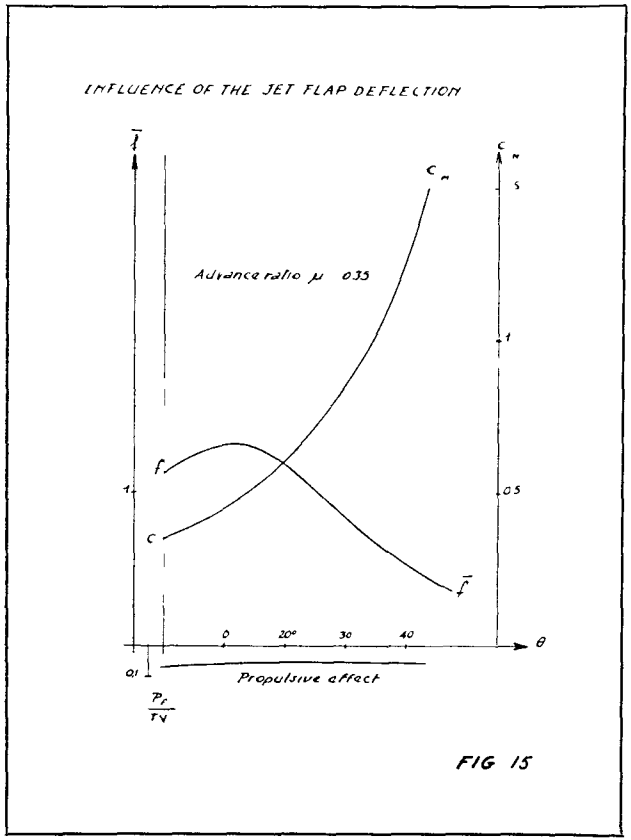

TABLE

FLIGHT CONDITIONS AT OPTIMUM ROTOR LIFT DRAG RATIO

CONFIGURATION		CONVENTIONAL NOZZLE			SLOTTED NOZZLE			JET FLAP CONTROL		
Flight { Helicopter / Gyrodyne	H / G	H	G	G	H	H	H	H	H	G
Advance ratio	λ	02	03	04	02	03	04	03	04	05
Relative lift drag ratio	f	008	108	035	084	11	11	14	14	12
Relative horizontal force	$\frac{F_x}{F_z}$	-05	+004	+006	-010	-003	0	-0,08	-005	0
C_L mean value		043	05	05	05	045	03	065	058	05

HELICOPTER FLIGHT		FLIGHT CONDITIONS AT MAXIMUM ROTOR PROPULSIVE								
CONFIGURATION		CONVENTIONAL NOZZLE			SLOTTED NOZZLE			JET FLAP CONTROL		
Advance ratio	λ	02	03		02	03		03	04	0,5
Relative lift drag ratio	$\bar{f}$	033	04		06	08		1	1	07
Relative horizontal Force	$\frac{F_x}{F_z}$	-018	-010		-028	-020		-023	-0,15	-01
C_L mean value	C_{L_H}	028	02		036	025		03	043	035

FIG 16

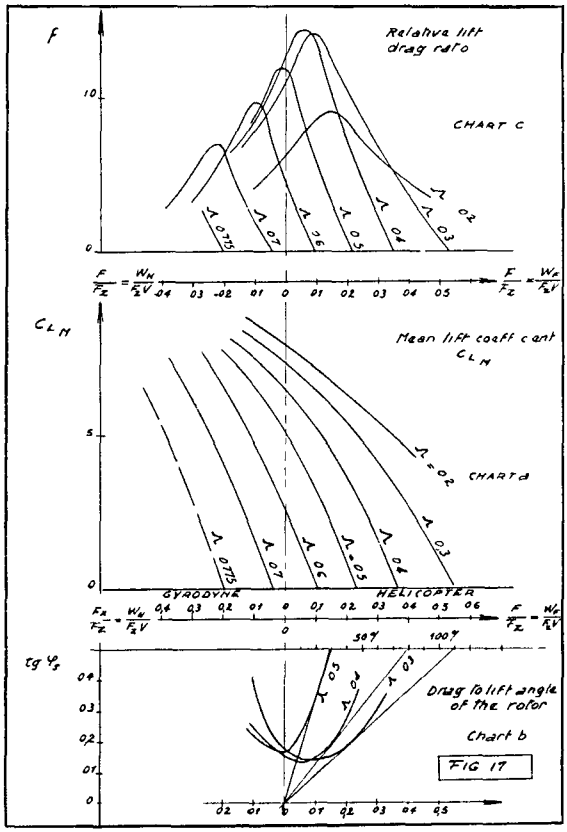

https://doi.org/10.1017/S2753447200004704 Published online by Cambridge University Press

Power corrections The air intake drag which has not been measured in the laboratory is to be added, in the designs, to the parasite drags The rotor power W_R, calculated according to the tests, is that which would be supplied by the driving fluid in hovering flight, which simplifies the power transmission computation without affecting its value

Application of Jet Flap Control to Transport Rotorcraft

The need to examine preliminary design studies

The predicted aerodynamic improvements shown earlier foreshadow gains in the field of " door-to-door " transport These gains can be estimated only in the light of tentative designs of machines provided with a fluid pressure generating plant fully adapted to the supply of the jet slots

It is important to make a certain number of tentative designs to take into account various compromises limiting the range of application of blown profiles if one does not want to be led to over-optimistic conclusions neglecting the limitations imposed by the fluid circulation in the blade This is why seven tentative designs have been envisaged within a speed range between 210 and 400 K p h and belonging to classes 2 and 3 among rotorcraft as defined earlier

Importance of the distance likely to be covered by thermal jet driven helicopters equipped with jet flap control The graph (Fig 18) shows that in transports along routes of about 500 Km the thermal jet driven rotor helicopter equipped with jet flap control may be expected to challenge the helicopter with mechanical transmission Our purpose is to study more closely the transport qualities

General characteristics of the projects

All-up weight The all-up weight is 10 tons in all designs and the

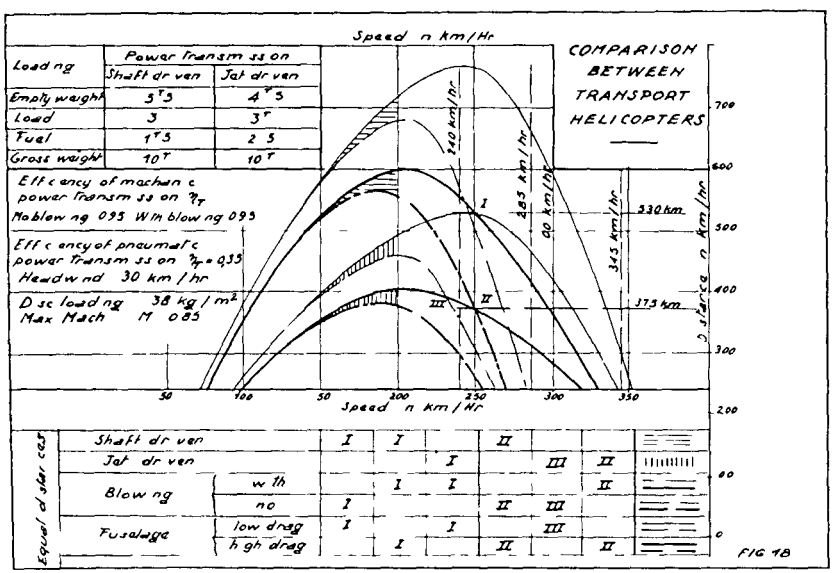

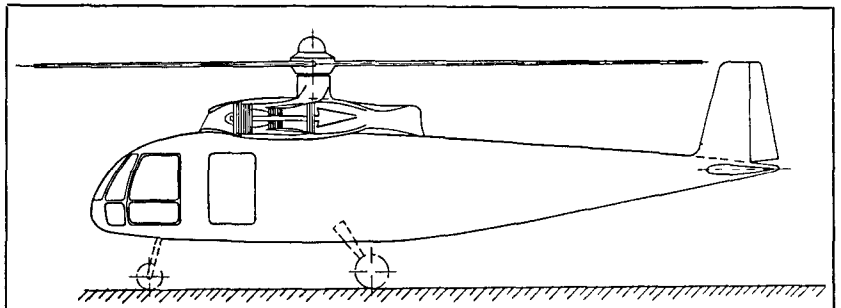

FIG 19

number of installed seats corresponds to the same transport performance (10^4 seat Km per hr) which leads to a reduction in fuselage volume and its drag as well as in the number of seats installed in the fastest aircraft (the number of seats varies from 50 to 30)

Outline of the helicopter (Fig 19) Slim fuselage with retractable landing gear and suitably finned to ensure directional stability and pitching attitude in forward flight Steering is obtained in hovering flight by actuating the vertical fin disposed within the ejection zone of the gas generating unit

Driving fluid generating plant Fig 20 illustrates by way of example a diagram of a three-flow generating plant similar to the CONWAY double flow unit This type is suitable for class 2 rotorcraft

Cold flow (L P compressor) and hot flow (large expansion turbine discharge) The ejecting velocity must be slow, both flows contributing to the fuselage propulsion at a moderate speed (320 K p h) and providing the yawing control

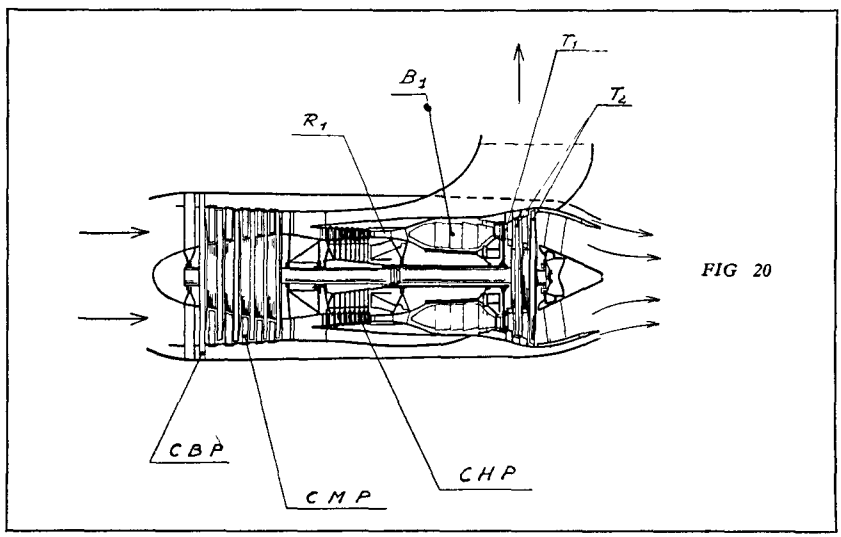

FIG 20

https://doi.org/10.1017/S2753447200004704 Published online by Cambridge University Press

Medium pressure cold flow feeding the ejection slots of the blades (medium pressure compressor) When changing from project I to project VII, the pressure ratio, P_T/P_0 of the blade feeding fluid varies from 3 5 to 1 8 A pressure ratio between 2 5 and 3 is advisable for Class 2 helicopters, the latter being the most economic

In the case of Classes 3 and 4 rotorcraft, a hot flow generating unit is to be used (same fluid characteristics as in NAPIER-ORYX)

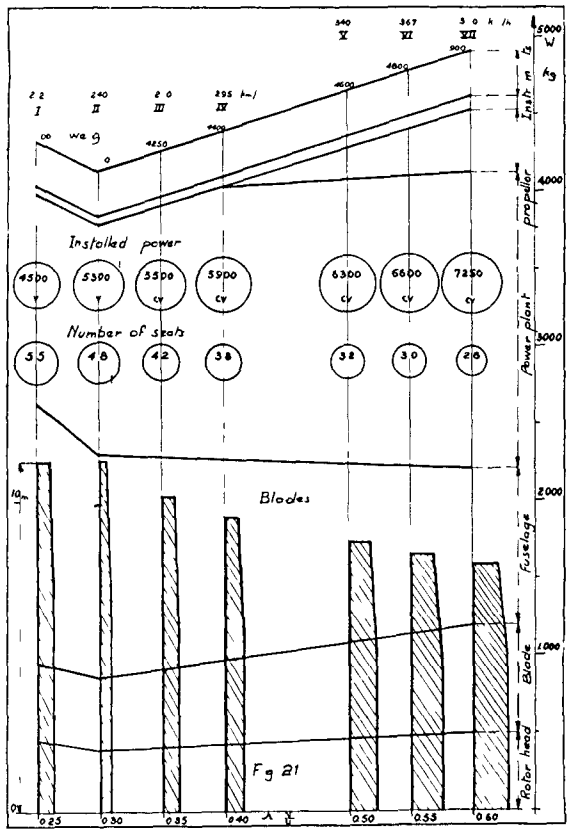

Dimensions of the three-bladed rotor (Diameter D, chord length l of the blade at $r = 6$)

The thickness ratio of the blades (from 20% up to $\bar{r} = 6$) progressively decreases towards the blade tip, the local Mach number being taken into account

Weight of the parts The graph (Fig 21) shows, for each project, a plan view of one blade and the weight table for each part

Aerodynamic characteristics The diagram showing the aerodynamic properties is essential for appreciating the effect of the jet flap control

The graph (Fig 22) gives, for each project, numbered from I to VII the aerodynamic properties as a function of the advance ratio

https://doi.org/10.1017/S2753447200004704 Published online by Cambridge University Press

The cruising speeds V associated with Λ values of each project, all correspond to the same Mach number $M = 85$ common to all designs, at the tip of the advancing blade The peripheral speed is therefore $U = 290$ m/sec $-V$

The aerodynamic properties distinguishing the various projects are stated below

Disc-loading $\frac{F_Z}{S}$ (curve A) The disc-loading $\frac{F_Z}{S}$ increases from 25 Kg/sq m to 50 Kg/sq m from project I to project VII due to the increase of the installed power

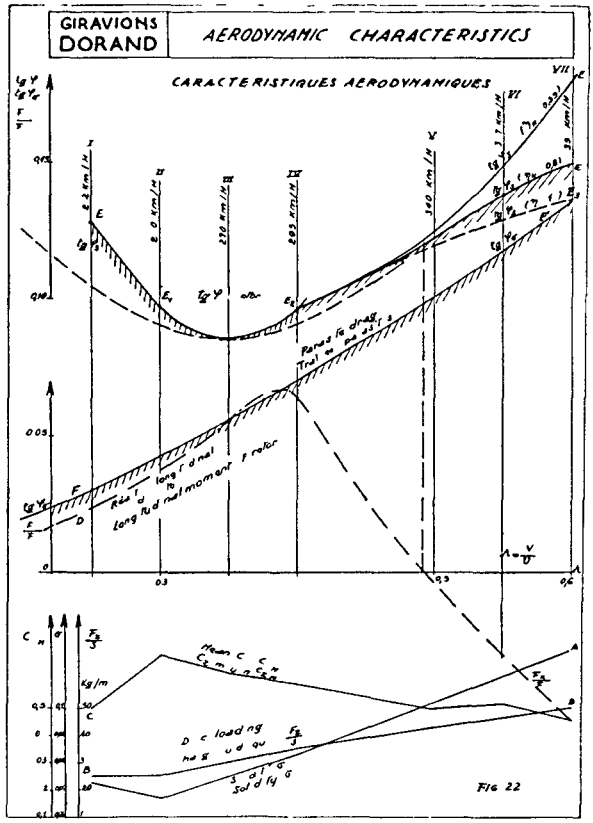

The vertical flight performance is, in fact, the same for all designs which have the same all-up weight of 10 tons

Mean C_L C_{L_M} (curve C) The mean C_L increases from project I ($C_{L_M} = 5$) which is not equipped with jet flap control to project II which embodies one ($C_{L_M} = 7$)

The mean C_L decreases from project II to project VII, from $C_{L_M} = 7$ to $C_{L_M} = 5$

Solidity σ (curve B) When changing from project II to project VII

https://doi.org/10.1017/S2753447200004704 Published online by Cambridge University Press

the increase of the disc-loading and the reduction of the mean C_L (C_{L_M}) lead to increases of the solidity σ, which is changed from 034 (project II) to 143 (project VII)

Horizontal force F_X (curve D) The horizontal propulsive force of the rotor increases from project I to project IV ($\Lambda = 4$) (flight in helicopter condition) It decreases in gyrodyne flight with auxiliary propeller Self-propulsion of the rotor takes place in project V ($\Lambda = 5$)

The rotor is pulled (projects VI and VII) for values of Λ higher than 5 (Fr Λ 0)

Lift/drag ratio of the rotor tan φ_S (curve E) The optimum lift/drag ratio ($\tan\varphi_S = 085$) occurs in project II ($\Lambda = 35$)

Beyond $\Lambda = 4$ (project IV) the shape of the curve E_1, E_2, rising towards the right, shows that it is advantageous to help the rotor in propelling the fuselage

In the case of the gyrodyne condition (projects V, VI and VII) the numerator of the ratio $\tan\varphi_S$ represents the sum of the powers supplied on the one hand to the rotor for producing the lift and on the other hand to the propeller for pulling the rotor alone

The denominator represents the product $F_Z V$ This remark explains the presence of the three sections E_2 E_3, E_2 E_4, E_2 E_5, graduated in terms of the efficiency η_H of the propeller

Relative parasite drag

The ratio $\tan\varphi_\sigma$ is defined by the relation

$$\tan\psi_\sigma = \frac{F_G}{F_Z}$$

(F_σ parasite drags)

This curve does not have the shape of a parabola since the fuselage volume decreases when changing from project I to project IV for the operational reasons mentioned earlier and further emphasized below

Remarks In order to counterbalance all the forces projected on the speed vector it is required to take into account not only the parasite drag F_σ but also the air intake drag and the residual thrust of the turbine, not measured in the laboratory This is why in helicopter flight (projects I to IV) the curve representing $\tan\varphi_\sigma$ does not exactly coincide with that representing $\frac{F_X}{F_Z}$

At low speeds, the effect of the residual thrust exceeds that of the air-intake drag (project I)

At higher speeds the reverse is true (projects between III and IV)

At a still higher speed (project IV), a low-pressure cold flow replenishment from the generating unit is required When changing from design III to design IV it becomes necessary to use the 3-flow generating unit

In projects I to III the low pressure coldflow is superfluous A 2-flow generating unit suffices

Feeding of the jet flap and pneumatic power transmission

Pressure ratio of the driving fluid The diagram of Fig 23 first shows, by way of illustration, the variation for each project of the pressure ratio of the driving fluid (curves A_1 and A_2)

In each project the pressure ratio decreases when changing from vertical flight (curve A_1) to horizontal cruising flight which requires a lower rate of flow of the fluid owing to the power reduction (curve A_2)

The pressure ratio, whose average value is about 2 5 to 3, decreases from project I to project VII, owing to the increase of the blade chord length l (curve B_1) which permits sending into the blade structure a larger fluid volume

The pressure ratio 1 75 permits using a hot flow generating unit of the NAPIER-ORYX type Two flow turbo-jet engines (GE CJ 805-21—General Electric or RB 141/3 (Rolls-Royce) may be envisaged

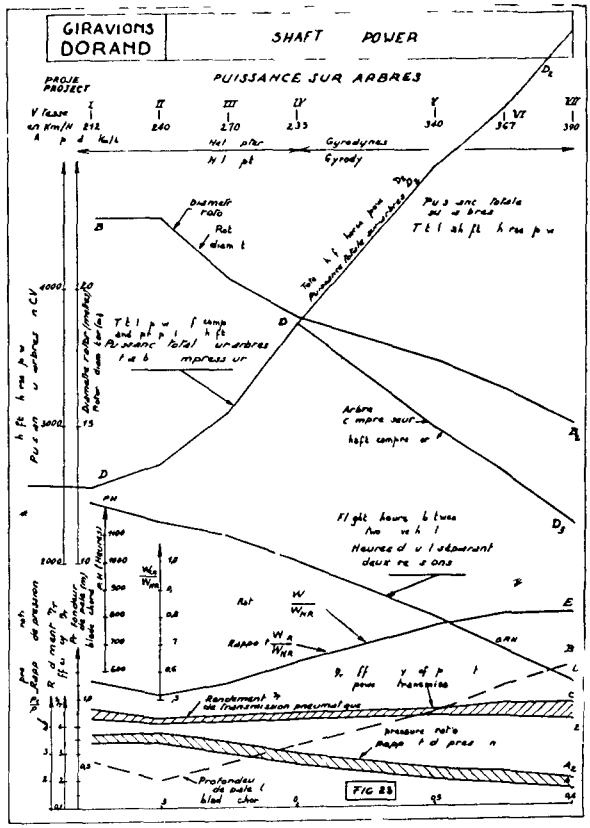

Efficiency of the pneumatic power transmission η_T

Curves C_1, C_2 show in the case of cold flow the variation of η_T with the flight condition (curve C_1 cruising condition—Curve C_2 vertical flight condition)

η_T increases when changing from project II to project VII owing to a reduction of the internal circulation speed in the wider blades and the reduction of the ejection velocity (lower pressure) which reduces the external losses

Total power to compressor shaft and propeller (curves D, D_1, D_2)

Compressor shaft power (curves D, D_1, D_3)

Propeller shaft power Difference between the preceding powers

https://doi.org/10.1017/S2753447200004704 Published online by Cambridge University Press

Overhaulıng of the turbınes ın the workshops Ratıo between the cruısıng power and the ' normal ratıng ' power Curve E Thıs ratıo makes ıt possıble to state from statıstıcs, the overhaul perıod of the turbınes (references 5 and 6)

The OP curves represent the number of flight hours between two successıve overhauls the knowledge of whıch ıs necessary for computıng the maıntenance cost OP drops down from 1,200 hours to 550 hours from project I to project VII

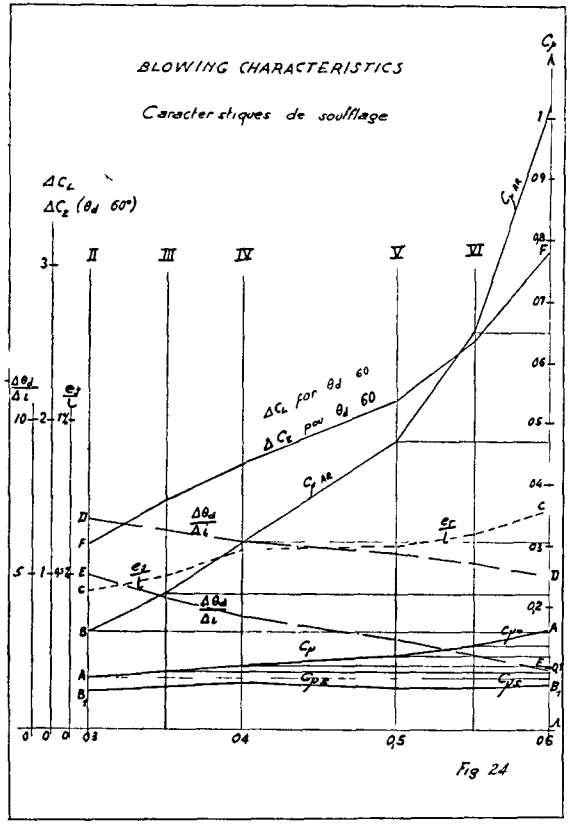

The dıstance flown between two successıve overhauls ıs on the average 200,000 km ın all projects due to the ıncrease of the speed V, notwıthstandıng the fall ın the overhaul perıod

Blowing Through the Trailing Edge

Momentum coefficient $C\mu$ The graph of Fıg 24 gıves the value of the momentum coefficıent $C\mu$ of the ejected fluıd ın the case of a slot wıth a wıdth proportıonal to $\bar{\tau}$

Vertıcal flıght Curve A gıves $C\mu$

Horızontal flıght Curve B gıves $C\mu_S$ of the blade passıng through the plane of symmetry whıch permıts computıng $C\mu$ ın all other azımuths for the varıous radıı (notatıons and formulae)

https://doi.org/10.1017/S2753447200004704 Published online by Cambridge University Press

Curve B_1 represents the coefficient $C\mu_{AR}$ of the retreating blade for $\bar{r} = 8$

Thickness α_j of the slot compared with the chord l (in %) Curve C giving $\frac{\alpha_j}{l}$ for $\bar{r} = 8$

Effectiveness of the flap deflection $\Delta\theta d$ compared to an incidence variation Δi $\frac{\Delta\theta d}{\Delta i}$

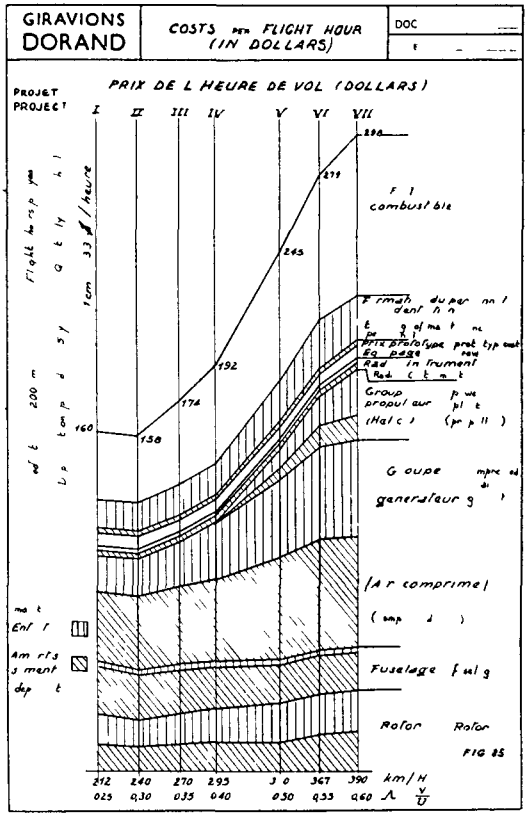

This ratio represents the number of degrees of flap deflection equivalent to an incidence variation of 1°

Case of hovering flight—Curve D On the average, a deflection $\Delta\theta d$ of about 5° is equivalent to an incidence variation of 1°

Case of the retreating blade—Curve E (section at $\bar{r} = 8$)

$\frac{\Delta\theta d}{\Delta i}$ varies from 5 (project II) to 2 (project VII) owing to the reduction of the air speed resulting from the increase of the advance ratio Λ with the speed

Curve F embodies the lift increase ΔC_L resulting from a 60° deflection of the retreating blade jet flap (ΔC_L increases from 1 2 to 3)

https://doi.org/10.1017/S2753447200004704 Published online by Cambridge University Press

Operating Cost

Hourly costs The diagram of Fig 25 indicates the hourly cost of flying corresponding to the various headings, the cost of each element being in turn split into depreciation, hourly cost (shaded areas) and maintenance costs (vertically shaded areas)

The computation method defined in Ref 6 has been simplified in the following way

The 'block' speed taking into account climb and descent has been replaced by V — 30 K p h, taking into account a head wind of 30 K p h

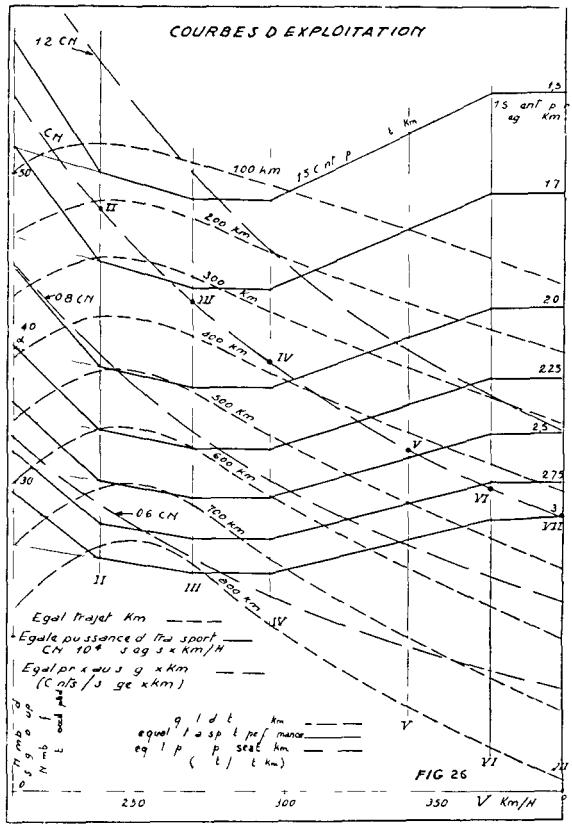

Remarks The cost of the power plant very rapidly increases with the speed, when changing from project I to project VII for which the hourly cost of the power plant represents 2/3 of the total hourly cost

The power plant is assumed to consist of turbines driving compressors

It should be pointed out that the future developments in the field of gas generating units will permit reducing the operating cost of the fastest aircraft

Operational Efficiency Diagram

Explanation of the Diagram The diagram of Fig 26 has as abscissae the cruising speed of the aircraft and as ordinates the number of passengers

in each flight It relates to the case of a power plant using existing elements The chain dotted curves constitute the ' transport capacity,' *i e*, the number of passenger Km transported per hour

Curve C N on which the project numbers are indicated represents the normal transport capacity with all seats occupied (10^9 passenger Km per hr) (normal loading = C N)

The curves 6 C N and 8 C N relate to the case when the seats are but partly occupied, the aircraft carrying more fuel to balance the total weight of 10 tons

Curve 1 2 C N corresponds to the case of the maximum transport capacity with supplementary seats or freight (mixed loading) (one passenger being replaced by 100 Kg freight)

The fuel weight is reduced, the total weight at the start being 10 tons in each case The dotted curves are those corresponding to equal distances They are graduated in Km The dotted lines join the points corresponding to the same cost per seat Km of the seven projects They are graduated in U S cents/passenger Km

Discussion of the Diagram

Range of the crane helicopters The range between projects I and II 212 to 240 Kp h yields the minimum transport cost for distances smaller than 300 Km 1 7 U S cent per passenger seat Km or 17 cents per ton Km It is the range of the " crane " helicopters For the same distance, the cost per passenger seat rapidly decreases with the speed reduction of 0 5 from project I to project II Machines flying at less than 240 K p h are therefore to be eliminated as regards passengers transportation, for distances above 300 Km

Range of economical transport The range between projects II and IV (speed varying from 240 K p h to 270 K p h) is particularly well adapted for stage lengths as great as 500 Km Price 2 censt per seat Km over 500 Km

Range of faster transport with high transport capacity The range included between projects IV and V (speed varying from 270 to 340 K p h) corresponds to more rapid machines with larger transport capacity Price 2 5 cents per seat Km over 500 Km The operational costs of the faster machines are burdened with the cost of the power plant which can be improved (cf next paragraph)

Remarks Project I is the only one that does not embody jet flap control That explains the break in the curve of cost per passenger seat

The jet flap control, in the case of project I, would be represented by the thin line segments shown on the left of the diagram between project I and II The price per seat Km would be, for example, 2 cents over 400 Km with jet flap control instead of 2 25 cents without same, as shown by α

Cost and Transport Capacity over the Same Stage Length as a Function of Speed With and Without Improved Power Plant

Explanation of the diagram (Fig 27) The top curves show the price of the passenger seat while the lower curves relate to the transport efficiency in the following three cases

Curves A Power unit making use of existing equipment

https://doi.org/10.1017/S2753447200004704 Published online by Cambridge University Press

Curves B Special gas generator of the future, according to sketch (Fig 2) including the following improvements

Weight reduction owing to grouping of turbines and compressors 20%

Price reduction 30%

Overhaul period 1,200 flight hours in all cases instead of 1,200 to 600 hours when changing from Project I to Project VII

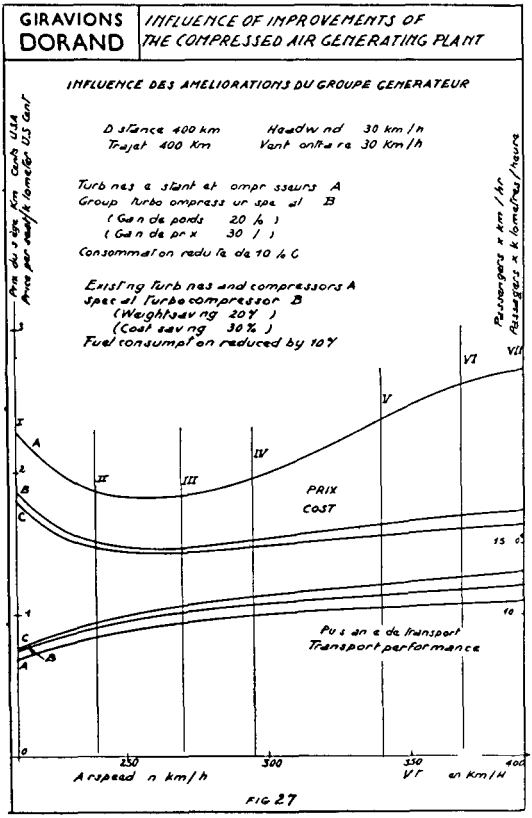

Curves Cα Special gas generator of the future, with additional improvement consumption reduced by 10%

Discussion of the diagram The price per passenger seat drops to a minimum in the vicinity of project III (speed 270 K p h) in the case of present-day power plants However, it varies but slightly from project III to project VII in the case of special gas generating units The consumption reduction has but a negligible effect In all the cases, the cost increases very quickly as the speed drops below 240 K p h (changing from project II to project I)

The transport capacity increases in all cases with the speed and benefits

from the improvements of the generators to a less pronounced degree than the cost per seat Km

Remarks The cost of the gas generator varies with the fluid characteristics the price per adiabatic horse-power is on the average of 28 $/G H P Apparently it may be reduced to 10 $/G H P for two-flow generators of 30,000 G H P

The operational costs shown based on evaluations of tentative projects give an approximate comparison of the various solutions Moreover, the price per seat Km increases as the weight decreases from 2 cents in the case of 35 passengers it would rise to 3 3 cents for a small 5–seat helicopter

Conclusions

Technical conclusions

The substitution of jet flap control for the conventional blade angle control as applied to rotorcraft with a thermal-jet driven rotor ensures the following improvements

Simplification of the rotor head and the blade articulations which remain at a fixed pitch

Servo-control requiring no effort

Possibility of flying faster without resorting to an auxiliary propulsive airscrew

Improvement of the rotor lift/drag ratio as well as the rotor propulsive power

Lowering of the vibration level and reduction of the alternating stresses in the blades during fast flight

Possibility of increasing the blade loading (C_{L_M} increased) as well as flying up to 390 K p h without resorting to ancillary fixed lifting surfaces

Design Conclusions

Transport of passengers by helicopter over 400 Km The study leads to envisage a pure helicopter of a speed between 280 and 350 K p h provided with a driving fluid generator supplying two flows (projects II and III) or three flows (project IV)

A flow with a medium pressure ratio (P_1/P_0 comprised between 2 5 and 3) and with high rate of flow feeding the ejection slots of the blades

Low exhaust speed ensuring yaw control in hovering flight (air flow over the vertical fin) and contributing to the propulsion (Fully expanded hot air escaping out of the turbine in the case of a helicopter flying between 280 and 300 K p h)

An additional low-pressure ratio cold flow(P_1/P_0 below 1 15) in the case of helicopters with a not very narrow fuselage or intended to fly between 300 and 350 K p h

Passenger transport over 400 Km by gyrodyne The future development of turbo-engines will permit a fast gyrodyne flying at 390 K p h and provided with a propelling airscrew In the neighbourhood and beyond this speed an auxiliary fixed surface is beneficial It permits reducing the ' solidity ' σ of the rotor

Crane helicopter The jet flap control would permit transport of heavy

loads over 200 to 300 Km under economical conditions at a cruising speed of about 250 K p h

Economic Conclusions

Slowness of present helicopters is expensive a speed below 220 K p h already leads to excessive cost In the case of existing power plants, the optimum operational cost corresponds to a speed between 270 and 320 K p h , for passenger helicopters, and a speed of about 250 K p h for thermal-jet driven crane helicopters

It is to be hoped that in the future the development of power plants will permit adopting a higher economical speed (350 K p h to 400 K p h) as well as increasing the transport capacity in the case of the ' gyrodyne ' configuration (case of an auxiliary propeller)

Notations and Formulae

This part of the paper aims at permitting the specialists to discuss the analysis with the help of the documents mentioned in the Appendix

Aerodynamic Quantities

Rotor diameter	D
Blade Chord Length	l
Number of Blades	b
Solidity	σ
Distance r between a profile element and the rotor axis	$\bar{r} = \frac{r}{R}$
Advance ratio	Λ
Rotorcraft forward speed	V
Rotor peripheral speed	U m/s
Angular velocity (radians/second)	ω
Vertical rotor thrust	F_Z
Horizontal rotor force	F_X
Mean C_L of the rotor	$C_{L_M} = \frac{3f_Z}{\sigma}$
Rotor thrust coefficient	f_Z

$$\frac{F_Z}{S} = \frac{P}{2} U^2 \bar{f_Z}$$

Swept disc area	S
Disc loading	$\frac{P}{S}$
Blade pitch angle	θ_C
Rotor shaft power	W_R
Rotor shaft power coefficient	$\tan \varphi_R = \frac{W_R}{F_Z V}$
Blade azimuth angle	ψ

ψ measured in the direction of the rotary motion from the blade as it passes through the plane of symmetry at the rear of the rotorcraft

https://doi.org/10.1017/S2753447200004704 Published online by Cambridge University Press

Case of the driving rotor

Propulsive force supplied by the rotor F_X

Relative propulsive force supplied by the rotor $\tan \varphi_F$

$$\tan \varphi_F = \frac{F_X}{F_Z}$$

Propulsive power supplied by the rotor W_F

$$W_F = \tan \varphi_F \times F_Z V$$

Lifting power and propulsive power of the rotor proper W_S

$$W_S = W_R - W_F$$

Draglift ratio of the rotor $\tan \varphi_S = \frac{W_S}{F_Z V} = \tan \varphi_R - \tan \varphi_F$

Lift/drag ratio of the rotor $f = \frac{1}{\tan \varphi_S}$

Case of the driven rotor

Power required by the rotor from the power plant (shaft power) W_H

$$W_H = \frac{F_X V}{\eta_H}$$

η_H power plant efficiency

Lift/drag ratio of the rotor and propellers together

$$\tan \varphi_S = \frac{W_R + W_H}{F_Z V} = \tan \varphi_R + \frac{1}{\eta_H} \frac{F_X}{F_Z}$$

Remarks In the case of the test results related to the rotor model DH-G 5, η_H has been taken equal to 0 6 which is an intermediate value between the efficiency of a propulsive airscrew and that of a fluid power plant with low ejection speed

Parasite drag (fuselage and rotor head) $T\sigma$

Relative parasite drag $\tan \varphi_\sigma$

$$\tan \varphi_\sigma = \frac{T\sigma}{F_Z}$$

https://doi.org/10.1017/S2753447200004704 Published online by Cambridge University Press

Thermodynamic characteristics

Shaft power of the compressor feeding the rotor with compressed air W_C

(case of cold flow)

$$W_C = \frac{W_R}{\eta_T}$$

nr efficiency of compressed air power transmission

$$0\,42 < \eta_T < 0\,48$$

Adiabatic efficiency of the flow discharged by the hot fluid generator Wa_g

Power transmission efficiency η_{T_a}

$$\eta_{T_a} = \frac{W_R}{W_{a_g}}$$

Ejection speed at the generator outlet for zero speed of the rotorcraft V_{J_g}

Ejection speed behind the trailing edge slots at a distance r from the rotor axis $V_{J_{\bar{r}}}$

Relative radius $\bar{r} = \frac{r}{R}$

Local circumferential speed $U_{\bar{r}}$

$$U_{\bar{r}} = \bar{r}U$$

Air intake efficiency (conventional definition) η_e

$$\eta_e = 0\,9$$

Air intake drag T_e

$$T_e = \frac{Q_p V}{g}$$

Q_p Weight (mass) flow of the fluid

g acceleration due to gravity

Basis of the simplified thermodynamic computation

Propulsive jet component

$$T = \frac{J_V}{2}\,(1 + \cos\theta_d)$$

$$J_V = \frac{Q_P}{g}\,V_{J_V}$$

V_{J_V} translatory ejection speed

$$V_{J_V}^2 = V_{J_g}^2 + U_F^2 + \eta_c \frac{V^2}{2g} - V_{J_V}^2 \left[A \left(\frac{V_c}{V_{J_0}} \right)^2 + B \right]$$

https://doi.org/10.1017/S2753447200004704 Published online by Cambridge University Press

$\eta_C = 0\ 90$ air intake efficiency

V_C internal circulation speed

$A \left(\frac{V_C}{V_{Jo}}\right)^2$ friction losses

B losses in the pipe-elbows and inlet diffuser

Instantaneous power supplied to a blade element

$$\Delta W_{h_1} = \frac{\Delta Q_P}{g} \left(\frac{V_{J_V}}{2} (1+\cos\theta_d) - \bar{U}\right) \bar{U}$$

Elementary drag due to the power plant

$$\Delta F_d = \frac{\Delta Q_{P_o}}{g} V - \frac{\Delta Q_{P_o}}{g} \left[\frac{V_{J_V}}{2} (1+\cos\theta_d) - U_{\bar{r}}\right] \sin\psi$$

Blowing air characteristics

Conventional momentum coefficient $C\mu$

$$\frac{Q_P V_J}{g} = \frac{\rho}{2} S_a V_a^2 C\mu$$

S_a airfoil provided with slot for air blowing

V_a local air speed

Definitions particularly concerning the rotor

The blowing air slot is progressively flaring from 0 6 R to the blade tip

Hovering flight The momentum coefficient $C\mu_0$, in hovering flight, is assumed to be constant, for a given radius, to make the definition of its value easier

In these conditions, the slot width increases with the square of the radius

Translational flight The momentum coefficient $C\mu$ varies according to the blade position, which is defined by the azimuth angle ψ (counted from the backward direction of the aircraft)

$$C\mu = \frac{C\mu_o}{(\bar{r} + \lambda \sin\psi)^2} \qquad C\mu_o = 2\frac{P_J}{P_z} \left(\frac{V_J}{u}\right)^2 \frac{S_J}{l}$$

Advancing blade	$\sin\psi = 1$	$C\mu_{AV}$
Retreating blade	$\sin\psi = -1$	$C\mu_{AR}$

https://doi.org/10.1017/S2753447200004704 Published online by Cambridge University Press

Coefficient $\frac{dC_L}{di}$ with effect of blowing

Value adopted in the computation

$$\frac{dC_L}{di} = 2\pi + \pi\sqrt{C_\mu}$$

The angle of incidence i is expressed in radians

Increment ΔC_L *of the* C_L *coefficient* in response to a jet flap deflection θd expressed in radians

$$\Delta C_L = K\, C_\mu{}^n\, \theta d$$

In the case of the relevant rates of flow the following values of K and n have been adopted

For the jet controls (from $\bar{r} = 0\,6$ to $\bar{r} = 0\,8$)

$K = 5\,3$ $\qquad$ $n = 1/2$

For the jet flap (from $\bar{r} = 0\,8$ to $\bar{r} = 1$)

$K = 3$ $\qquad$ $n = 1/2$

Remarks In the case of the tests of rotor DH-G 5, the jet reflection was constant from $\bar{r} = 0\,7$ to

$\bar{r} = 0\,86$, it was controlled only from

$\bar{r} = 0\,86$ to $\bar{r} = 1$

In the case of the projects under consideration, it would be interesting to study also flap control from $F = 0\,6$ to $F = 1$

The above performances have been obtained without these future improvements They are deduced from test results and take into account corrections of solidity σ and profile drag C_{Dp}

C_{Dp} has been taken equal to 0 0125

References

Ref 1-A *ASSOCIATION TECHNIQUE MARITIME ET AERONAUTIQUE*, Jan, 1955
"Hypersustentation et pilotage des avions par controle de circulation," by Ph POISSON-QUINTON and P JOUSSERANDOT
This statement sums up the results of the fundamental experimental survey under flat flow, at the Saint-Cyr INSTITUT AEROTECHNIQUE and undertaken by the OFFICE NATIONAL D'ETUDES ET DE RECHERCHES AERONAUTIQUES (ONERA) in co-operation with the SERVICE TECHNIQUE AERONAUTIQUE and Societe "GIRAVIONS DORAND"

Ref 1-B "Essais systematiques d'hypercirculation par soufflage au bord de fuite d'un profil NACA 0018 en incompressible" (Jan, 1955) *Onera Technical Notice*, 2/1727-A
Testing effected by the OFFICE NATIONAL D'ETUDES ET DE RECHERCHES AERONAUTIQUES (ONERA) in co-operation with the SERVICE TECHNIQUE AERONAUTIQUE and Societe "GIRAVIONS DORAND"

Ref 1-C "Essais en ecoulement plan transsonique d'un profil avec soufflage pres du bord de fuite" (Jan, 1959) *Onera Technical Notice*, 4/1833-A
These tests relate to a DORAND jet deviator

REF 2 Docaero No 25 Jan , 1954
" Amelioration des qualites des voilures tournantes en translation par pilotage multicyclique " by R Dorand

REF 3-A Advanced Research Division of Hiller Helicopters
" Application of circulation Control to helicopters rotors,"
G J SISSINGH — R N GREENMAN — M G GOFFNEY — A H SACKS

REF 3-B *Journal of the American Helicopter Society* Vol 4, No 3, July, 1959
" Application of the jet-flap principle to helicopters,"
Rene DORAND — Gabriel D BOEHLER

REF 4 Congres International Aeronautique, Paris, June, 1959
" Application pratique du controle d'un rotor d'helicoptère par le volet de bord de fuite comportant le soufflage " Rene DORAND

REF 5 Transport Helicopters
" Operating Cost Analysis Methods (Hiller)

REF 6 " Design study of the feasibility of Flying-crane-type helicopters incorporating the jet-flap control system " Report No 1088—*Giravions Dorand*

REF 7-A Giravions Dorand, Patent of Invention (P V No 777,763, filed 10-29-58)
" Moyeu de rotor d'helicoptere rapide "

REF 7 Giravions Dorand, Patent of Invention P V No 777,595, granted on 10 27 58
" Perfectionnement aux organes de controle de voilures tournantes "

REF 7-C Giravions Dorand, Patent of Invention P V No 777,596, granted on 10 27 58
" Perfectionnements technologiques aux procedes de déviation de nappes fluides ejectees par le bord de fuite des pales d'helices ou d'ailes "

REF 7-D Giravions Dorand, Patent applied for
" Moyeu d'helicoptere a rotor souffle "

REF 8 3rd European Aeronautical Symposium (Bruxelles, 1958)
" Application comparee de la propulsion par tuyères d'ejection disposees au bord de fuite de profil de voilures dans le cas de l'avion STOL ou de l'helicoptere " by R DORAND

REF 9 Patents granted to Societe GIRAVIONS DORAND, concerning the generation and circulation of the operating fluid as well as thermo propelled rotors control including blowing
9-A — U S Patent No 2 650 666, allowed on 7/16/47
9-B — British Patent of Invention No 634 332, allowed on 7/18/47
o-C — Canadian Patent No 498 532, granted on 12/15/1953

REF 10 Power plants

REF 10-A Communication to the Association Technique et Aeronautique (Science et Technique Aeronautiques), June, 1947
" Distances franchissables comparees d'helicopteres comportant divers types d'installations motrice "

Ref 10-B Communication at the first French symposium on gyrodynes
" Giravions a rotors thermopropulses par fluide moteur à basse pression "

REF 11 " Simulateur de vol d'helicopteres," by R Dorand (Science et Technique Aeronautiques)